A high-fidelity heralded quantum squeezing gate

Jie Zhao[1,6], Kui Liu[2,6], Hao Jeng[1], Mile Gu[3,4,5], Jayne Thompson[5], Ping Koy Lam [1✉] and Syed M. Assad [1]

Squeezing operation is critical for continuous-variable quantum information, enabling encoding of information in phase space to a resolution otherwise forbidden by vacuum noise[1]. A universal squeezing gate that can squeeze arbitrary input states is particularly essential for continuous-variable quantum computation[2,3]. However, the fidelity of existing state-of-the-art implementations is ultimately limited due to their reliance on first synthesizing squeezed vacuum modes of unbounded energy[4,5]. Here, we circumvent this fundamental limitation by using a heralded squeezing gate. This allows improved gate fidelity without requiring more squeezed ancillary vacuum. For a specific target squeezing level for coherent states, we present measured fidelities higher than what would be possible using non-heralded schemes that utilize up to 15 dB (ref. [6]) of best available ancilla squeezing. Our technique can be applied to non-Gaussian states and provides a promising pathway towards high-fidelity gate operations and fault-tolerant continuous-variable quantum computation.

Gaussian operations are essential building blocks for continuous-variable quantum information processing. With the exception of the squeezing operation, all other Gaussian operations can be readily realized with near unit fidelity in quantum optics. However, the current capability to implement squeezing operations with high fidelity remains limited. This is unfortunate, because the squeezing operation is a prerequisite for universal quantum computation[2,3]. It is also a necessary component for many other fundamental quantum operations like the controlled-Z gate[7–9], the quantum non-demolition gate[10], the control phase gate[11] and quantum error correction[12]. Moreover, its application to non-Gaussian states facilitates quantum information tasks such as decoherence mitigation[13], preparation of non-classical states[14] and quantum state discrimination of coherent-state qubits[15].

Although extensive effort has been devoted to the generation of squeezed vacuum[6,16], the development of a universal squeezing gate that can act on arbitrary input states has been lagging behind. Recent experiments have successfully generated a squeezed vacuum with a squeezing magnitude of 15 dB (ref. [6]). In contrast, demonstrations of a universal squeezing gate have only attained 1.2 dB for a reliable fidelity of 94% (refs. [17,18]). High squeezing levels for vacuum inputs are possible through the parametric amplification process in an optical cavity. However, extending this method to arbitrary input states presents substantial challenges due to cavity loss[14,19,20] and interference effects[21,22].

Instead, current state-of-the-art implementations of a universal squeezing gate use an ancillary squeezed vacuum as a resource to drive the squeezing gate[4,5,17,18]. Once the ancillary state has been prepared, the squeezing gate can be implemented using Gaussian measurements and feed-forward operations. However, highly squeezed ancilla are required to achieve a reasonable fidelity. Unit fidelity can only be achieved with an infinitely squeezed ancilla. Thus, in realistic implementations, the output fidelity will always be limited.

Here, we present and experimentally demonstrate a heralded squeezing gate that overcomes this limitation. A heralding filter is implemented in the feed-forward operation, whereby an enhancement in fidelity can be achieved by increasing the filter strength without requiring more squeezing resources. In contrast to conventional implementations, this scheme can approach unit fidelity. With the inclusion of the present squeezing gate, we thus have a complete set of Gaussian operations that can be implemented with high fidelity.

The universal squeezing gate performs the unitary operation $S(r_t) = \exp\left[\frac{1}{2}(r_t^\star a^2 - r_t a^{\dagger 2})\right]$, where a is the annihilation operator and r_t is the target squeezing strength. Our squeezing gate is illustrated in Fig. 1. First, an optical parametric amplifier is used to produce an ancillary squeezed vacuum with squeezing parameter r_a. Next, an input state ρ_{in} is mixed with the ancillary state on a beamsplitter with transmissivity t_s. The reflected mode is then split on a beamsplitter with transmissivity t_m so that its amplitude and phase quadratures can be measured simultaneously. The measurement outcome, denoted by a complex number α_m, is used to herald a successful squeezing operation by employing a probabilistic filter. The gate is successfully heralded with the following probability (see Methods):

$$P_f(\alpha_m) = \begin{cases} \exp\left[\left(1 - \dfrac{1}{g_f}\right)(|\alpha_m|^2 - \alpha_c^2)\right] & \text{for} \quad |\alpha_m| < \alpha_c \\ 1 & \text{for} \quad |\alpha_m| \geq \alpha_c \end{cases} \quad (1)$$

This filter function, which was previously used to emulate a noiseless linear amplifier[23–25], depends on two parameters: the filter strength $g_f \geq 1$, and the cutoff parameter α_c. A large filter strength will result in a higher output fidelity at the expense of a lower success probability. When $g_f = 1$, the heralded squeezing gate reduces to the conventional squeezing gate. The cutoff parameter determines the operational regime; a larger cutoff will allow for the squeezing of states with a higher mean photon number. Finally, with a successful heralding event, the measurement outcomes of amplitude and phase are rescaled by the electronic gains g_x and g_y, and fed forward to the transmitted mode to complete the squeezing operation. The target squeezing level is determined by

[1]Centre of Excellence for Quantum Computation and Communication Technology, Department of Quantum Science, Research School of Physics and Engineering, The Australian National University, Canberra, Australian Capital Territory, Australia. [2]State Key Laboratory of Quantum Optics and Quantum Optics Devices, Institute of Opto-Electronics, Collaborative Innovation Center of Extreme Optics, Shanxi University, Taiyuan, China. [3]School of Physical and Mathematical Sciences, Nanyang Technological University, Singapore, Singapore. [4]Complexity Institute, Nanyang Technological University, Singapore, Singapore. [5]Centre for Quantum Technologies, National University of Singapore, Singapore, Singapore. [6]These authors contributed equally: Jie Zhao, Kui Liu. ✉e-mail: ping.lam@anu.edu.au
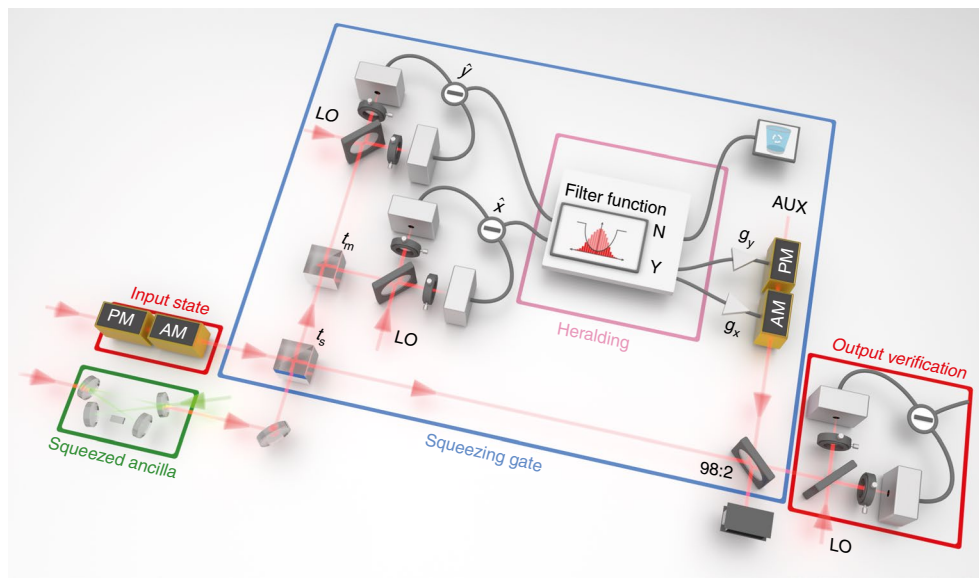
Fig. 1 | Experimental layout of the heralded squeezing gate. The gate is composed of three parts. First, the input state and an ancillary squeezed vacuum are prepared. Second, the two states are mixed on a beamsplitter with transmissivity t_s. The reflected part of the input state is sent to a dual homodyne measurement where the two conjugate quadratures, amplitude $\hat{X}$ and phase $\hat{Y}$, are measured with a split of t_m. This measurement, in conjunction with a heralded filtering function, feed-forwarding and a displacement operation, constitute the core of our probabilistic squeezing gate. Finally, a verification homodyne is employed to characterize the squeezed output. Transmissivities t_s and t_m can be tuned to obtain a trade-off between fidelity and success probability. By setting $t_m = 1$ in our experimental demonstration, we obtain a higher success probability compared to the dual homodyne set-up, without much degradation in the fidelity. AM/PM, electro-optic amplitude/phase modulators; LO, local oscillator; AUX, auxiliary beam.
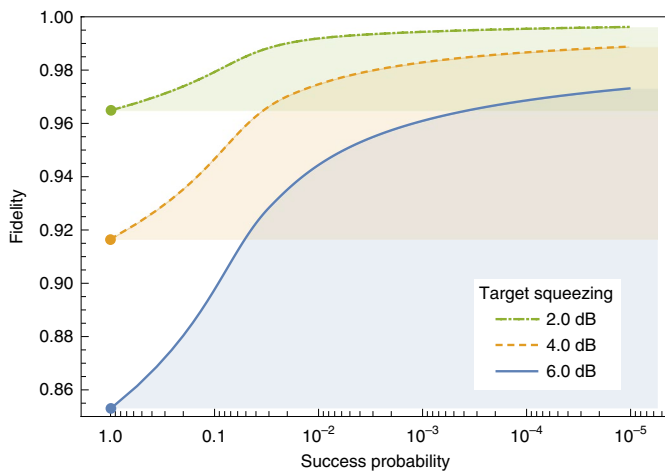

Fig. 2 | Fidelity against success probability for various target squeezing values. Starting with a pure squeezed ancilla of 6 dB, the fidelity is plotted as a function of success probability for three values of the target squeezing: 2 dB, 4 dB and 6 dB. The shaded area represents the accessible operational regime of the presented squeezing gate. For comparison, the fidelity of a conventional deterministic squeezing gate is superimposed (filled circles). In all cases, a substantial enhancement in fidelity is achieved with the heralded squeezing gate, at the expense of a lower success probability. The cutoff α_c is chosen to include more than 98% of the total statistics to ensure the Gaussianity of the output is preserved (Supplementary Section 4).

Fig. 3 | Phase-space diagram for the squeezing gate. To verify the phase invariance of the squeezing operation, five coherent states (A–E), located at different regions of phase space, were chosen as inputs. The target squeezings are 2.30 dB, 4.81 dB, 5.84 dB, 8.85 dB and 10.16 dB, respectively. The corresponding inputs, the experimental and the desired squeezed outputs are represented by the noise contours (1 s.d. width) of their Wigner functions. In all circumstances, the squeezing gate behaves consistently, irrespective of the input amplitude or phase.

the ancillary squeezing level and the transmissivity of the two beamsplitters (Supplementary Section 1).

The faithfulness of a squeezing gate is typically benchmarked by the fidelity between the output and ideal target state. For Gaussian inputs within the operational regime, this fidelity is independent of the input quadrature amplitudes. This is because
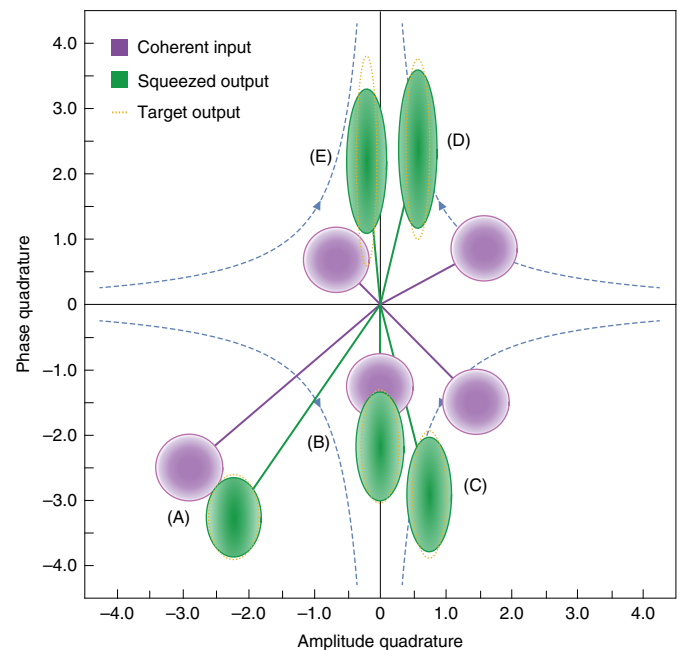
we operate at the unity gain point where the mean quadrature amplitudes of the output and target coincide (Supplementary Section 1).
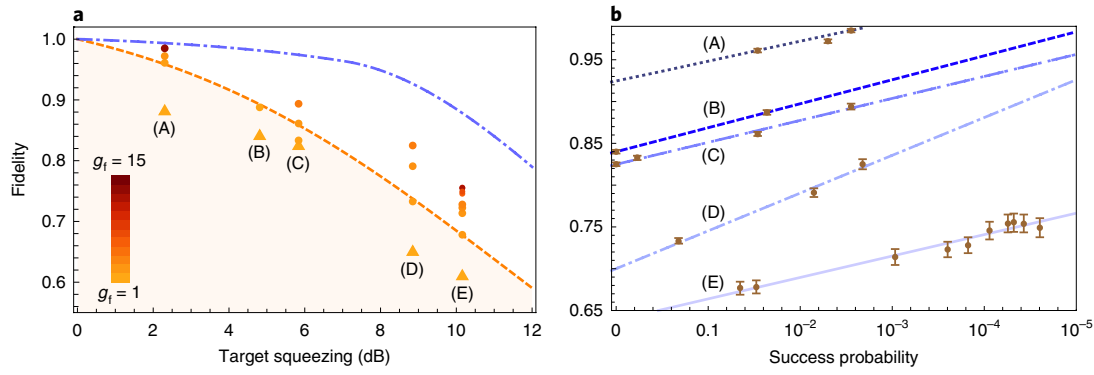
Fig. 4 | Improvement in fidelity over conventional techniques for a series of target squeezing values for states A–E. a, The optimal fidelities attainable in two scenarios are plotted as performance benchmarks: the presented squeezing gate when a dual homodyne is performed (top blue dash-dotted curve) and a conventional squeezing gate (bottom orange curve). Both lines assume no experimental imperfections, representing the optimal fidelity attainable from our initial squeezed resource. Experimental results with target squeezing between 2.30 dB and 10.16 dB are plotted as filled circles and show an increase in fidelity as the filter strength increases (darker gradient colour). Filled triangles show the fidelity obtained when the filter strength is set to one. **b**, The improvement in fidelity comes at the expense of decreasing success probability. Error bars represent 1 s.d. of the output fidelity (Supplementary Section 3).
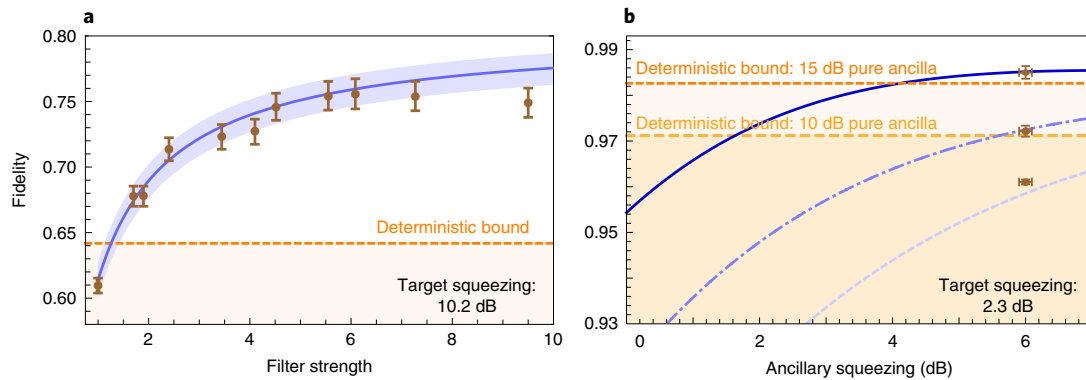

Fig. 5 | Fidelity as a function of filter strength and ancillary squeezing. a, The fidelity increases consistently with a higher filter strength, which agrees with the theoretical prediction taking into account experimental imperfections (blue shaded region). The orange dashed line denotes the limit of fidelity for deterministic protocols assuming pure 6 dB squeezed ancilla and perfect experimental conditions. Reaching fidelity beyond this would require a larger amount of ancillary squeezing conventionally. **b**, Filter strength can compensate ancillary squeezing strength. The requirement for a more squeezed ancilla can be circumvented with the presented squeezing gate. The three blue lines, from bottom to top, represent filter strengths of $g_f = 1.52$, 3.38 and 12.63. For comparison, we present the achievable fidelity for a conventional squeezing gate operating with the currently best available squeezing of 15 dB (dashed dark orange line) and 10 dB squeezing (dashed light orange line), but sustaining the same in-loop detection efficiency as is present in our set-up. With 6 dB of initial squeezing, we observe fidelity surpassing both bounds. Error bars represent 1 s.d. of the output fidelity and the ancillary squeezing.

Figure 2 illustrates the trade-off between fidelity, target squeezing and success probability. We identify two operational regimes distinguished by the filter strength. When the filter strength is low, we operate in the first regime, which exhibits a favourable success probability. The majority of fidelity enhancement can be obtained without dropping below 1% success probability. Regardless of the target squeezing, a substantial improvement in fidelity is obtained compared to the conventional approach. In the second regime, a high filter strength allows near unit fidelity for any target squeezing $r_t \leq r_a$, which is impossible conventionally. An attractive feature of our scheme is that we can choose to operate in either regime by simply tuning the filter strength without reconfiguring the experimental set-up.

We now report the experimental results. An auxiliary squeezed vacuum with 6.0 dB squeezing and 6.5 dB anti-squeezing was used as a resource to drive the squeezing gate. In the experiments, we performed a single quadrature measurement by setting $t_m = 1$. This allowed for a higher success probability compared to a dual quadrature measurement, while maintaining comparable fidelity enhancement. In this case, the transmissivity t_s was set according to $t_s = e^{-2r_t}$

(Supplementary Section 1). To test the squeezing gate, we prepared several coherent input states and characterized their outputs by performing homodyne measurements on the amplitude and phase quadratures. We implemented at least 10^6 runs for each input state to generate enough statistics.

First, we present the results for five input states with different phases and with magnitudes $|\alpha_{in}|$ ranging from 0.70 to 1.92 (Fig. 3). The target squeezing for these states varies between 2.3 dB to 10.16 dB. A true squeezing gate operates on arbitrary inputs irrespective of their amplitude or phase. This was verified by the measured outputs of our squeezing gate.

Second, we characterize the fidelity as a function of target squeezing in Fig. 4a. The best conventional output fidelity attainable in an idealized experiment using the same ancillary resource but assuming no loss is plotted as a benchmark. We show that this benchmark can be surpassed by increasing the filter strength without requiring a more squeezed ancilla. The trade-off between fidelity and success probability is illustrated in Fig. 4b. For most runs, the success probabilities are greater than 10^{-4}.

Third, Fig. 5a illustrates the relationship between fidelity and filter strength. The continuous increase in fidelity as a function of filter strength agrees with the theoretical model accounting for experimental imperfections (for a detailed analysis see Supplementary Section 4 and Supplementary Fig. 7). The deterministic limit is plotted to identify the minimum filter strength required to exceed this benchmark. We clearly surpass this benchmark for all the datasets.

Finally, Fig. 5b showcases the performance of the heralded squeezing gate in the high-fidelity regime when the filter strength is increased to 12.63. For an input magnitude of $|\alpha_{in}| = 2.91$ and target squeezing of 2.3 dB, we measured a fidelity of 0.985 ± 0.001. This fidelity cannot be achieved with the current best squeezed resource[6] in the conventional scheme subject to the same homodyne detection efficiency. Assuming idealized experimental process with zero loss, obtaining this fidelity would require a pure 10.5 dB squeezed ancilla.

In conclusion, we propose and experimentally demonstrate a heralded squeezing gate that achieves near unit fidelity for coherent inputs while requiring only modest ancillary squeezing. Crucially, heralding circumvents the requirement for a highly squeezed ancilla as is necessary in conventional methods. The trade-off between fidelity and success probability can be tuned at will, and the majority of fidelity improvement can be achieved without the success probability dropping below 1%. This methodology enables us to synthesize squeezing gates to a fidelity that would otherwise be impossible for conventional schemes, even with a pure and infinitely squeezed ancillary resource subject to the same experimental loss. In doing so, our techniques complete the set of all Gaussian operations that can be experimentally performed with high fidelity.

There are a number of situations where trading determinism for high-fidelity squeezing can be useful. Notably, in Supplementary Section 2 we show that our techniques can be adapted to squeeze non-Gaussian states, such as the single-photon state and the Schrödinger's cat state, with near unit fidelity. This provides a feasible pathway to creating exotic non-classical states[26], which are key resources for computation and engineering sophisticated nonlinear evolutions[27,28]. High-amplitude cat states, for example, are critical to certain models of universal continuous-variable computation[29,30]. In the cluster state setting, such non-classical states constitute a resource that enables a continuous-variable cluster to perform computations that cannot be efficiently simulated classically[2,3,31]. Here, such resources only need to be prepared offline, and a non-deterministic mechanism for synthesizing them merely adds an overhead to the preparation procedure. Furthermore, in quantum sensing[29,30] and illumination, the most physically pertinent resource cost is often the number of photons sent. For example, each probe risks damaging the sample in biological sensing[32], while in covert sensing, each probe risks detection by an adversary[33]. In such scenarios, it becomes quite reasonable to pay a heavier cost during state preparation to maximize the efficacy of each probe. Each of these possibilities merits investigation, whereby one can ascertain the extent to which it is worthwhile to trade determinism for high fidelity.

Online content

Any methods, additional references, Nature Research reporting summaries, source data, extended data, supplementary information, acknowledgements, peer review information; details of author contributions and competing interests; and statements of data and code availability are available at https://doi.org/10.1038/s41566-020-0592-2.

References

1. Weedbrook, C. et al. Gaussian quantum information. *Rev. Mod. Phys.* **84**, 621 (2012).
2. Mile, G., Weedbrook, C., Menicucci, N. C., Ralph, T. C. & van Loock, P. Quantum computing with continuous-variable clusters. *Phys. Rev. A* **79**, 062318 (2009).
3. Menicucci, N. C. Fault-tolerant measurement-based quantum computing with continuous-variable cluster states. *Phys. Rev. Lett.* **112**, 120504 (2014).
4. Miyata, K. et al. Experimental realization of a dynamic squeezing gate. *Phys. Rev. A* **90**, 060302 (2014).
5. Ukai, R. et al. Demonstration of unconditional one-way quantum computations for continuous variables. *Phys. Rev. Lett.* **106**, 240504 (2011).
6. Vahlbruch, H., Mehmet, M., Danzmann, K. & Schnabel, R. Detection of 15 dB squeezed states of light and their application for the absolute calibration of photoelectric quantum efficiency. *Phys. Rev. Lett.* **117**, 110801 (2016).
7. Menicucci, N. C., Ma, X. & Ralph, T. C. Arbitrarily large continuous-variable cluster states from a single quantum nondemolition gate. *Phys. Rev. Lett.* **104**, 250503 (2010).
8. Braunstein, S. L. Squeezing as an irreducible resource. *Phys. Rev. A* **71**, 055801 (2005).
9. Yurke, B. Optical back-action-evading amplifiers. *J. Opt. Soc. Am. B* **2**, 732–738 (1985).
10. Yoshikawa, J.-I. et al. Demonstration of a quantum nondemolition sum gate. *Phys. Rev. Lett.* **101**, 250501 (2008).
11. Puri, S. & Blais, A. High-fidelity resonator-induced phase gate with single-mode squeezing. *Phys. Rev. Lett.* **116**, 180501 (2016).
12. Braunstein, S. L. Error correction for continuous quantum variables. *Phys. Rev. Lett.* **80**, 4084–4087 (1998).
13. LeJeannic, H., Cavailles, A., Huang, K., Filip, R. & Laurat, J. Slowing quantum decoherence by squeezing in phase space. *Phys. Rev. Lett.* **120**, 073603 (2018).
14. Miwa, Y. et al. Exploring a new regime for processing optical qubits: squeezing and unsqueezing single photons. *Phys. Rev. Lett.* **113**, 013601 (2014).
15. Takeoka, M. & Sasaki, M. Discrimination of the binary coherent signal: Gaussian-operation limit and simple non-Gaussian near-optimal receivers. *Phys. Rev. A* **78**, 022320 (2008).
16. Andersen, U. L., Gehring, T., Marquardt, C. & Leuchs, G. 30 years of squeezed light generation. *Phys. Scr.* **91**, 053001 (2016).
17. Yoshikawa, J.-I. et al. Demonstration of deterministic and high fidelity squeezing of quantum information. *Phys. Rev. A* **76**, 060301 (2007).
18. Su, X. et al. Gate sequence for continuous variable one-way quantum computation. *Nat. Commun.* **4**, 2828 (2013).
19. de Oliveira, F. A. M. & Knight, P. L. Bright squeezing. *Phys. Rev. Lett.* **61**, 830–833 (1988).
20. LaPorta, A., Slusher, R. E. & Yurke, B. Back-action evading measurements of an optical field using parametric down conversion. *Phys. Rev. Lett.* **62**, 28–31 (1989).
21. Zhang, J., Ye, C., Gao, F. & Xiao, M. Phase-sensitive manipulations of a squeezed vacuum field in an optical parametric amplifier inside an optical cavity. *Phys. Rev. Lett.* **101**, 233602 (2008).
22. Ma, H., Ye, C., Wei, D. & Zhang, J. Coherence phenomena in the phase-sensitive optical parametric amplification inside a cavity. *Phys. Rev. Lett.* **95**, 233601 (2005).
23. Fiurášek, J. & Cerf, N. J. Gaussian postselection and virtual noiseless amplification in continuous-variable quantum key distribution. *Phys. Rev. A* **86**, 060302 (2012).
24. Chrzanowski, H. M. et al. Measurement-based noiseless linear amplification for quantum communication. *Nat. Photon.* **8**, 333–338 (2014).
25. Zhao, J., Hao, J. Y., Symul, T., Lam, P. K. & Assad, S. M. Characterization of a measurement-based noiseless linear amplifier and its applications. *Phys. Rev. A* **96**, 012319 (2017).
26. Laurat, J., Coudreau, T., Treps, N., Matre, A. & Fabre, C. Conditional preparation of a quantum state in the continuous variable regime: generation of a sub-Poissonian state from twin beams. *Phys. Rev. Lett.* **91**, 213601 (2003).
27. Andersen, U. L., Neergaard-Nielsen, J. S., van Loock, P. & Furusawa, A. Hybrid discrete- and continuous-variable quantum information. *Nat. Phys.* **11**, 713–719 (2015).
28. van Loock, P. Optical hybrid approaches to quantum information. *Laser Photon. Rev.* **5**, 167–200 (2011).
29. Ralph, T. C. Coherent superposition states as quantum rulers. *Phys. Rev. A* **65**, 042313 (2002).
30. Munro, W. J., Nemoto, K., Milburn, G. J. & Braunstein, S. L. Weak-force detection with superposed coherent states. *Phys. Rev. A* **66**, 023819 (2002).
31. Menicucci, N. C. et al. Universal quantum computation with continuous-variable cluster states. *Phys. Rev. Lett.* **97**, 110501 (2006).
32. Taylor, M. A. et al. Biological measurement beyond the quantum limit. *Nat. Photon.* **7**, 229–233 (2013).
33. Bash, B. A., Gagatsos, C. N., Datta, A. & Guha, S. Fundamental limits of quantum-secure covert optical sensing. In *Proc. 2017 IEEE Int. Symp. on Information Theory* 3210–3214 (IEEE, 2017).

Methods

Experimental details. As depicted in Fig. 1, the experiment consisted of four parts: a squeezed vacuum source, input preparation, a squeezing gate composed of homodyning and feed-forward, and a homodyne station for characterizing the output state. The main light source was a continuous-wave frequency-doubled Nd:YAG laser (Innolight Diablo), producing an ~300 mW fundamental wave at 1,064 nm and a 400 mW second-harmonic wave at 532 nm. The fundamental beam passed through a mode cleaner cavity with a finesse of 760 to further purify its spatial mode and attenuate the high-frequency noise of the laser output. The input coherent states were created by modulating the fundamental beam at 4 MHz sideband frequency using a pair of electro-optical modulators. The squeezed vacuum was prepared in a doubly-resonant bow-tie cavity where below-threshold optical parametric amplification (OPA) took place using a 10.7 mm potassium titanyl phosphate crystal periodically poled with 9 μm period. The front and rear surfaces of the crystal were superpolished and anti-reflection-coated with reflectivity $R < 0.1\%$ at 1,064 nm and $R < 0.2\%$ at 532 nm. Three intracavity mirrors were coated to be highly reflective at both 1,064 nm and 532 nm ($R > 99.99\%$ for the two concave mirrors and $R = 99.85 \pm 0.05\%$ for the flat mirror) and the input/output coupler had a customized reflection of $83 \pm 1\%$ at 1,064 nm and $73 \pm 1.2\%$ at 532 nm. Up to 11 dB squeezed vacuum could be generated with a bandwidth of ~36 MHz.

Special care was taken in the implementation of all phase locks throughout the experiment. The OPA cavity was locked on co-resonance with both the fundamental beam (1,064 nm) and the pump beam (532 nm) by means of the Pound–Drever–Hall technique, with a 11.25 MHz phase modulation on the pump. The same modulation signal was also utilized to lock the relative phase between the signal beam and the squeezed ancilla that is output from the OPA. The relative phase between the seed and the pump was carefully controlled using a phase modulation at 41.5625 MHz on the seed beam. We used this modulation to ensure that the OPA always operated at parametric de-amplification, yielding amplitude-squeezed vacuum. The interference between the seed and the local oscillators/auxiliary beam on each homodyne station was controlled similarly with an amplitude modulation (24.25 MHz) and phase modulation (30 MHz) on the signal beam, giving access to the measurement of an arbitrary quadrature angle.

In the experimental investigation of our squeezing gate, we concerned ourselves with five different coherent inputs, each assigned with a particular target squeezing. By setting $t_s = 1$, these input states were characterized by homodyne measurements on the amplitude and phase quadratures. The experimental parameters and measured results for the data depicted in Figs. 3–5 are provided in Supplementary Table 1.

Filter function. The filter function is used to determine if the squeezing gate operation is successful or not. This is accomplished by picking a random number from a uniform distribution between 0 and 1 and comparing that to $P_f(\alpha_m)$ (equation (1)), where α_m denotes the measurement outcome of the in-loop dual homodyne detection. The operation is heralded as successful when the random number is less than $P_f(\alpha_m)$. In this case, the measurement outcome is amplified and fed forward. Otherwise, the operation is considered to have failed and is aborted. The acceptance rate $P_f(\alpha_m)$ thus determines the likelihood of the acceptance of each outcome, which depends on the amplitude of the input, the filter strength and the cutoff. For an initial Gaussian distribution of α_m, the resultant distribution remains Gaussian provided that the cutoff is sufficiently large, but with its mean and variance both being amplified by g_f (ref. [25]). To be concrete, by applying the filter function on an unnormalized Gaussian ensemble with mean α_0

$$e^{-|\alpha_m - \alpha_0|^2} \tag{2}$$

the ensemble evolves according to multiplying equation (2) by the acceptance rate $P_f(\alpha_m)$. The output distribution is essentially a concatenation of two Gaussian distributions joined at the circle $|\alpha| = \alpha_c$. The inputs with $\alpha_m \geq \alpha_c$ are unaffected, whereas those with $\alpha_m < \alpha_c$ are filtered and become proportional to

$$e^{-|\alpha_m - \alpha_0|^2} e^{(1 - 1/g_f)(|\alpha_m|^2 - \alpha_c^2)} = \frac{e^{(g_f - 1)|\alpha_0|^2}}{e^{(1 - 1/g_f)\alpha_c^2}} \exp\left(-\frac{|\alpha_m - g_f \alpha_0|^2}{g_f}\right) \tag{3}$$

Note that only the second part (equation (3)) that undergoes post-selection is desired. Therefore, a sufficient cutoff should be able to embrace this Gaussian as much as possible. To be more explicit, it was proposed in ref. [25] that

$$\alpha_c = g_f^2 |\alpha_m| + \beta g_f \sigma_{\alpha_m} / \sqrt{2} \tag{4}$$

Here, σ_{α_m} is the standard deviation of the input distribution and β quantifies how well the cutoff circle embraces the output distribution. On restoring proper normalization of the output distribution, we obtain the success probability of the filtering operation as

$$P_s = \frac{e^{(g_f - 1)|\alpha_0|^2}}{\pi \ e^{(1 - 1/g_f)\alpha_c^2}} \iint_{|\alpha_m| < \alpha_c} \exp\left(-\frac{|\alpha_m - g_f \alpha_0|^2}{g_f}\right) d^2\alpha_m$$
$$+ \frac{1}{\pi} \iint_{|\alpha_m| \geq \alpha_c} \exp(-|\alpha_m - \alpha_0|^2) d^2\alpha_m \tag{5}$$

We note that a larger cutoff enables a wider operational range of the filter function, but at the expense of decreased success probability. For an input ensemble with a large amplitude, a sufficiently large α_c is required; otherwise, the part of the output distribution beyond α_c is subject to distortion[25]. Hence, α_c needs to be carefully tailored according to the input ensemble to ensure a faithful squeezing operation while still maintaining a reasonable probability of success (Supplementary Section 5).

Data availability
The data that support the plots within this paper and other findings of this study are available from the corresponding author upon reasonable request.

Author contributions
S.M.A., J.Z., M.G., J.T. and P.K.L. conceived the experiment. S.M.A. and J.Z. developed the theoretical model. J.Z., K.L., H.J., S.M.A. and P.K.L. planned and performed the experiment. J.Z. and S.M.A. analysed the data. J.Z., S.M.A., H.J., J.T., M.G. and P.K.L. drafted the initial manuscript. All authors discussed the results and commented on the manuscript.

Competing interests
The authors declare no competing interests.

Additional information
Supplementary information is available for this paper at https://doi.org/10.1038/s41566-020-0592-2.

Correspondence and requests for materials should be addressed to P.K.L.

Reprints and permissions information is available at www.nature.com/reprints.